Paper
Int'l J. of Aeronautical & Space Sci. 16(4), 548–559 (2015)
DOI: http://dx.doi.org/10.5139/IJASS.2015.16.4.548

IJASS
International Journal of Aeronautical and Space Sciences

Quasi-steady State Simulation of Rotating Detonation Engine

Mohammed Niyasdeen*

Pusan National University, Busan 46241, Republic of Korea

Sejong Oh, Kui Soon Kim** and Jeong -Yeol Choi*****

Pusan National University, Busan 46241, Republic of Korea

Abstract

We performed a numerical simulation based on the two-dimensional (2-D) unsteady Euler's equation with a single-step Arrhenius reaction model in order to investigate the detonation wave front propagation of an Argon (Ar) diluted oxy-hydrogen mixture ($2H_2 + O_2 + 12Ar$). This simulation operates in the detonation frame of reference. We examine the effect of grid size and the performance impact of integrated quantities such as mass flow. For a given set of baseline conditions, the minimal and maximum grid resolutions required to simulate the respective detonation waves and the detonation cell structures are determined. Tertiary shock wave behavior for various grids and pre-exponential factors are analyzed. We found that particle fluctuation can be weakened by controlling the mass flow going through the oblique shock waves.

Key words: Rotating detonation engine (RDE), pulse detonation engine (PDE), oblique shock waves, numerical simulation.

1. Introduction

Since the detonative propulsion research has obtained its peak [1-9], the practical application of such propulsive device is still a question mark (to authors' insight). The current focus in utilizing detonative propulsion for air-breathing engines has evolved from the pulsed mode to the continuous rotating mode. Pulsed operation is applicable to a flight Mach number up to about 3 to 4. In contrast, the concept of the Rotating Detonation Engine (RDE) is attractive for Mach numbers above 4. Pulse detonation engines (PDEs) designed for flight Mach numbers exceeding 3 to 4 have increased complexity and are becoming too expensive. Similarly, gas turbine engines also have some disadvantages when compared to the RDEs in terms of the engineering and materials used. In particular, gas turbines have reduced efficiency, increased cost, and delayed responses to changes in power settings.

Global interest in the development of RDEs for aerospace propulsion has led to numerous studies of detonative propulsion, particularly relating to efficiency. This is evident from the formation of collaborative teams and groups by universities and industries worldwide. Much of the early research was carried out to examine the gaseous detonative wavelet structure [10-19] and its typical cellular patterns [20]. Recently, Choi et al. [21] proposed a common standard of grid resolution prerequisites for achieving an explicit simulation of detonation cell structure in a 2-D rectangular channel. However, interest in the development of the RDE has led to various numerical and experimental investigations worldwide. Hishida et al. [22] numerically stabilized an orthodox rotating detonation front propagating at nearly the Chapman Jouguet (CJ) velocity. They determined that smaller cell sizes (3 to 3.5 mm) near the solid wall due to triple shock collision and larger cell sizes (4 mm) on the unconfined region. Until now, no detailed grid resolution study has been performed for an RDE to predict the minimum grid size for detonation wave formation and the fine grid size needed to resolve the detonation cell structures. In the present study, we attempted to clarify these issues. For a given set of baseline conditions, the coarse and fine grids required for producing their respective detonation wave

* Masters student
** Professor
*** Professor, Corresponding author: aerochoi@pusan.ac.kr

Received: July 27, 2015 Revised: November 23, 2015 Accepted: December 10, 2015

http://ijass.org pISSN: 2093-274x eISSN: 2093-2480

fronts, and the detonative cellular structures, were determined in order to provide guidance for future RDE studies. Moreover, we performed a quasi-steady state simulation (QSS) (body-fixed coordinates to wave-attached coordinates) as described in Section 3.3. Time-efficient performance calculations for determining the flow field characteristics of an RDE are the main benefit of using a QSS.

In terms of performance, when compared to conventional engines, an RDE has a high energy release rate and high thermodynamic efficiency. Following the pioneering work of Voitsekhovskii et al. [23, 24] and Nicholls et al. [25, 26], meticulous theoretical and experimental studies of RDEs were performed by Bykovskii et al. [27, 28]. In the last decade, Daniau et al. [29, 30] introduced the use of a liquid H_2 and O_2 mixture in RDEs for performance calculations. Davidenko et al. [8] simulated a rotating detonation in a 2-D unwrapped RDE chamber with the detailed chemical kinetics and higher-order schemes. Hishida et al. [22] performed a performance analysis with 70% argon-diluted H_2/O_2 compound. Hayashi et al. [31] suggested that the inlet pressure, temperature, and Mach number have a significant effect on rotating detonation device performance. Yi et al. [6] found that the propulsive performance is strongly dependent on the mass flowrate of an injected mixture, and weakly reliant on the axial chamber length and the number of detonation waves. Zhou and Wang [4] discussed the thermodynamic performance of continuously rotating detonation. Time-accurate calculations of a RDE were developed by Schwer and Kailasanath [32] at the Naval Research Laboratory--they suggest that the specific impulse relies on the pressure ratio, whereas the mass flow and propulsive force are primarily determined by the stagnation properties of the inlet micro-nozzles. Very recently, Aerojet Rocketdyne introduced a plasma augmentation system [33] to improve engine performance by continuing the air breathing operation without supplemental O_2. Despite the substantial progress achieved thus far in RDE performance investigations, questions remain concerning the performance dependency factor associated with flow particle fluctuations. The present work focused on some of the preliminary results of close - up view of the detonation wave front, temporal evolution of the pressure regularity, including non-uniform exhaust flow and the number of detonation wave fronts in the computational domain, to give a better idea of the particle dependency factor's effect on engine performance and insight into the flow field within the RDE.

This paper is organized as follows. We describe the basic mathematical formulation in Section 2. We then describe numerical simulation conditions that include the RDE physical modeling (Section 3.1) and the injection boundary conditions (Section 3.2). A brief outline of the quasi-steady state simulation procedure is given in Section 3.3. Our preliminary results are presented in Section 4.1, the grid test is described in Section 4.2, and the main results are given in Sections 4.3-4.5.

2. Mathematical Formulations

2.1 Governing equation and numerical method

The quasi-steady state analysis of a rotating detonation engine is obtained by applying 2-D unsteady Euler equations with a source term due to the chemical reaction for the $2H_2 - O_2 - 12Ar$ mixture.

$$\frac{\partial \vec{Q}}{\partial t}+\frac{\partial \vec{F}}{\partial x}+\frac{\partial \vec{G}}{\partial y}=\vec{S}$$

$$\vec{Q}=\begin{bmatrix}\rho\\ \rho u\\ \rho v\\ \rho E\\ \rho Y\end{bmatrix}\vec{F}=\begin{bmatrix}\rho u\\ \rho u^2+p\\ \rho uv\\ (\rho E+p)u\\ \rho uY\end{bmatrix}\vec{G}=\begin{bmatrix}\rho v\\ \rho uv\\ \rho v^2+p\\ (\rho E+p)v\\ \rho vY\end{bmatrix}\vec{S}=\begin{bmatrix}0\\ 0\\ 0\\ 0\\ \dot{\omega}\end{bmatrix} \quad (1)$$

A fourth-order Monotonic Upstream-Centered Scheme (MUSCL) Total Variation Diminishing (TVD)--based Roe scheme is used for the convective flux with one-step irreversible Arrhenius kinetics for the chemical reaction model, as described by Eq. (2):

$$\omega=\rho(1-Y)k\exp\left(\frac{-E_a}{p/\rho}\right) \quad (2)$$

$$T=\frac{p}{\rho R} \quad (3)$$

where k is the pre-exponential factor, E_a is the activation energy, Y is the reaction progress variable, ρ is the density, and p is the pressure. The required temperature (T) is then found through the equation of state as described by Eq. (3). Hereafter, all quantities displayed and discussed are nondimensional values.

3. Numerical Simulation Conditions

3.1 RDE physical modeling

A schematic of a three-dimensional (3-D) RDE is

illustrated in Fig. 1(a). The unwrapped 2-D RDE with a detonation wave front is shown in Fig. 1(b). This 2-D numerical simulation of the combustion chamber problem of concern involves azimuthal detonation wave propagation. A combustible fresh mixture is injected from the bottom end, and then the burnt gas moves out of the downstream exit. To avoid the need for a large computational domain to capture this process, a reference frame was designed as shown in Fig. 2. From the bottom end, the premixed stoichiometric $H_2 - O_2 - Ar$ fresh mixture is injected into the combustion chamber, where the flow field is initially at standard temperature and pressure conditions. The controlling parameters of the injected fuel are given in Section 3.2. Periodic boundary conditions are applied on the side faces (right and left sides). Supersonic outflow boundary conditions are imposed on the downstream exit of the computational domain.

3.1.1 Computational grids

The computational domain consists of a uniform dense grid in the upstream region for perfect shock wave capturing. A nonuniform stretched grid in the downstream region was used to reduce the computational cost and time. To further verifying the results, a grid resolution study was performed by varying the grid size, as summarized in Table 1.

3.1.2 ZND structure

The one-dimensional (1-D) Zel'dovich-Von Neumann-Doring (ZND) wave structure was applied as the initial condition for this 2-D simulation. A small rectangular-shaped 1-D CJ detonation wave front is kept in the middle portion of the azimuthal direction to provide the initial flow disturbances. With 1-D steady state assumptions, the conservation laws can be reduced to the following set of algebraic equations:

$$\rho_1 v_1 = \rho_2 v_2 \tag{4}$$

$$p_1 + \rho_1 v_1^2 = p_2 + \rho_2 v_2^2 \tag{5}$$

$$h_1 + q + \frac{1}{2} v_1^2 = h_2 + \frac{1}{2} v_2^2 \tag{6}$$

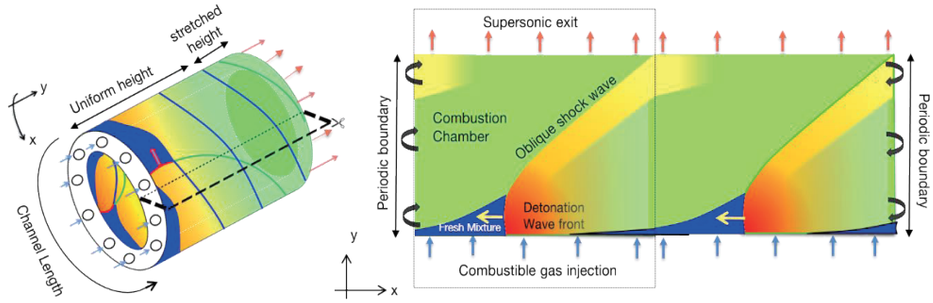

(a) (b)

Fig. 1. (a) Schematic of 3-D RDE chamber to (b) 2-D unwrapped RDE showing detonation

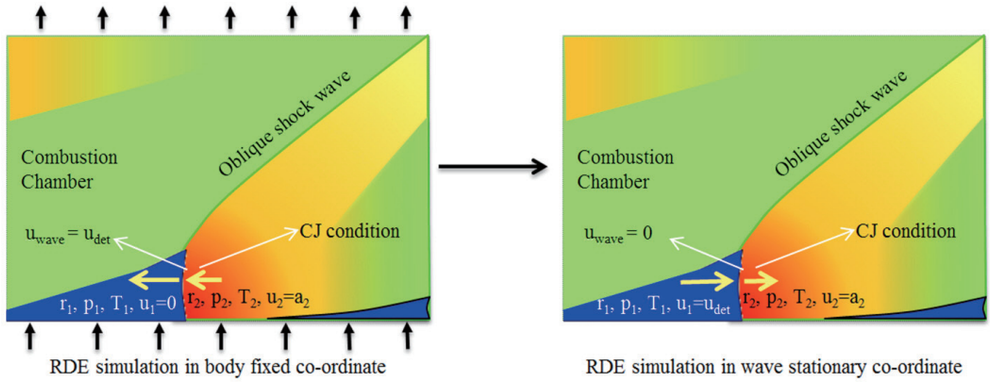

(a) (b)

Fig. 2. (a) Body-fixed coordinate to (b) wave-stationary coordinate.

DOI: http://dx.doi.org/10.5139/IJASS.2015.16.4.548

$$\frac{\rho_2}{\rho_1}=\frac{1+\gamma_1 M_1^2}{1+\gamma_2 M_2^2}\left(\frac{a_1}{a_2}\right)^2\left(\frac{\gamma_2}{\gamma_1}\right) \tag{7}$$

$$\frac{\rho_2}{\rho_1}=\frac{1+\gamma_1 M_1^2}{1+\gamma_2 M_2^2}\left(\frac{a_1}{a_2}\right)^2\left(\frac{\gamma_2}{\gamma_1}\right) \tag{8}$$

The pressure, density, and velocity can be derived as a function of the reaction progress variable, followed by the temperature through the equation of state as described by Eq. (3). Further simplification leads to Eq. (9), which gives the final CJ Mach number calculation:

$$M_{D,C\ J}=\left[\left(\frac{\gamma_2^2-1}{\gamma_1-1}q+\frac{\gamma_2^2-\gamma_1}{\gamma_1^2-\gamma_1}\right)+\sqrt{\left(\frac{\gamma_2^2-1}{\gamma_1-1}q+\frac{\gamma_2^2-\gamma_1}{\gamma_1^2-\gamma_1}\right)^2-\left(\frac{\gamma_2}{\gamma_1}\right)^2}\right]^{1/2} \tag{9}$$

3.2 Injection boundary conditions

The fresh stoichiometric mixture inflow is computed along the bottom end face of the combustion chamber. The stagnant properties for the pre-mixer were set at constant values; however, the inflow varies accordingly depending on the relationship between the stagnant and flow properties at the bottom end face. With the assumption of isentropic expansion through the downstream exit, three injection conditions are formulated in order to supply the fresh mixture.

1. For $p_w >= p_0$, no inflow:

$$p=p_w, T=T_0\left(\frac{p}{p_0}\right)^{\frac{\gamma-1}{\gamma}}, v=0 \tag{10}$$

2. For $p_0 > p_w > p_{cr}$, subsonic inflow:

$$p=p_w, T=T_0\left(\frac{p}{p_0}\right)^{\frac{\gamma-1}{\gamma}}, v=\sqrt{\frac{2\gamma}{\lambda-1}RT_0\left[1-\left(\frac{p}{p_0}\right)^{\frac{\gamma-1}{\gamma}}\right]} \tag{11}$$

3. For $p_w <= p_{cr}$, supersonic inflow:

$$p=p_c, T=T_0\left(\frac{p}{p_0}\right)^{\frac{\gamma-1}{\gamma}}, v=\sqrt{\frac{2\gamma}{\lambda+1}RT_0} \tag{12}$$

where γ, p_0, T_0 represent the specific heat ratio, total pressure, and total temperature, respectively. The critical pressure (P_{cr}) is defined in terms of the stagnant pressure as follows:

$$p_{cr}=p_0\left(\frac{2}{\gamma+1}\right)^{\frac{\gamma}{\gamma-1}} \tag{13}$$

For the injection conditions, density can be calculated from the equation of state (Eq. 3), energy can be calculated using Eq. (14), and the reaction progress is taken to be zero.

$$e=\frac{p}{\gamma}+\rho\left[\frac{1}{2}\left(u^2+v^2\right)\right]-\frac{q}{\gamma\times z} \tag{14}$$

3.3 Quasi-steady state solution procedure

Most previous RDE simulations have used body-fixed coordinates as shown in Fig. 2(a), whereas the moving reference frame (Fig. 2(b)) is rarely implemented because

Table 1. Summary of numerical simulation cases

Grid spacing	Minimum spacing
38 × 38 uniform grids – 38 × 31; stretched grids – 38 × 7	Δ x = Δ y = 0.08
76 × 76 uniform grids – 76 × 66; stretched grids – 76 × 10	Δ x = Δ y = 0.04
151 × 151 uniform grids – 151 × 136; stretched grids – 151 × 15	Δ x = Δ y = 0.02
301 × 301 uniform grids – 301 × 250; stretched grids – 301 × 51	Δ x = Δ y = 0.01
601 × 601 uniform grids – 601 × 550; stretched grids – 601 × 51	Δ x = Δ y = 0.005
1201 × 1201 uniform grids – 1201 × 1150; stretched grids – 1201 × 51	Δ x = Δ y = 0.0025
2001 × 2001 uniform grids – 2001 × 1950; stretched grids – 2001 × 51	Δ x = Δ y = 0.00125

of the difficulties in identifying the detonation speed. In moving reference frame simulations, it is very hard to define the detonation propagation velocity in terms of the CJ detonation speed. It is reasonable to use a moving reference frame because of its advantages, including time efficient calculations of performance and flow field characteristics.

The azimuthal velocity (u) is mentioned during the inflow, and it is here that the reference frame change is implemented. Rather than specifying u = 0 (which is the body-fixed coordinate), a particular detonation speed of 10% less than the CJ speed is prescribed instead. Because of this change to the detonation reference frame, the computational space becomes one in which a quasi-steady state is possible. This is the computational equivalent to placing a small backward-moving aircraft model in a wind tunnel and blowing the air rather than moving the model.

4. Results and Discussion

Our RDE numerical study was achieved using an H_2 – O_2 – Ar mixture. In this section, the preliminary results, and a quasi-steady state analysis, are described.

4.1 Preliminary numerical results

Before looking at the parametric investigation in detail, we first considered the basic typical solutions in order to acquire greater insight into RDE functioning, its performance, and the flow field characteristics. In this analysis, there is a small backward azimuthal propagation in the detonation wave front when the detonation velocity was limited to 10% less than the CJ detonation speed. In order to achieve a quasi-steady state simulation of the RDE, the initial detonation velocity was retained as 5.12 (nondimensional), which is 10% lower than the actual reference CJ detonation speed of 5.656 (nondimensional) with the dimensionalized reference parameter equivalent to 339.4 m/s. As mentioned previously, the exit boundary was fixed as a supersonic boundary, and in the downstream region, all conserved variables were extrapolated from only the interior grid points of the domain.

Figure 3 shows the general features of the RDE flow field. The detonation front (a) is propagating in the azimuthal direction near the head wall; the fresh premixed fuel is injected sub-sonically (b) and super-sonically (c) from the bottom end; oblique shock waves (e) formed due to the

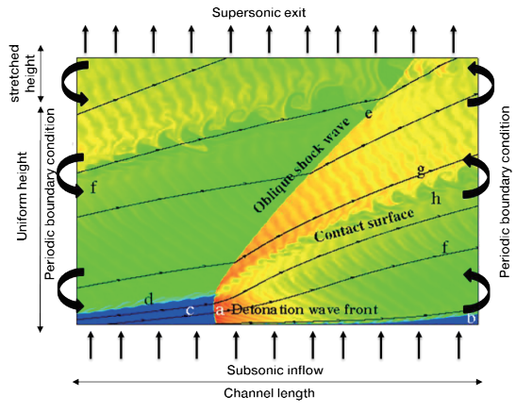

Fig. 3. Schematic of RDE annular chamber

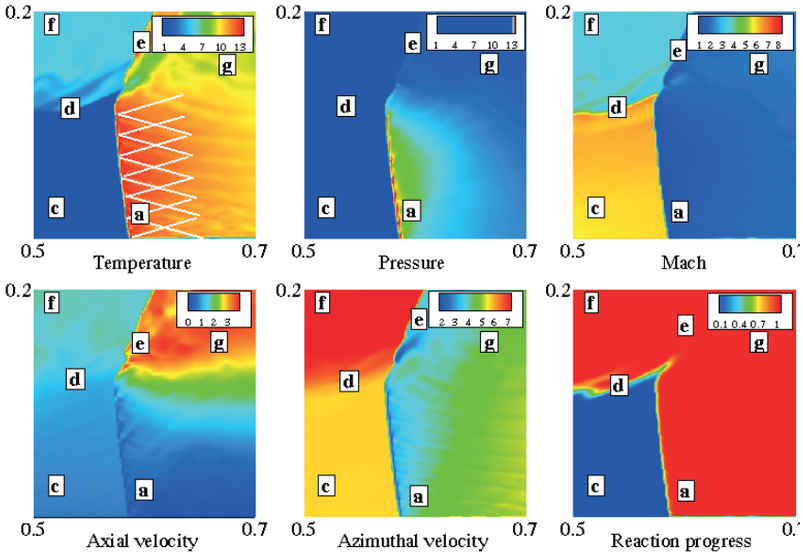

Fig. 4. Close-up view of various detonation properties of the flow field (using the same labeling and conditions as shown in Fig. 3).

DOI: http://dx.doi.org/10.5139/IJASS.2015.16.4.548

high speed flow mixing; a small instability criteria (d) can be seen in the mixing layer which obviously lead to some performance losses; the secondary shock wave region behind the detonation wave front varies considerably depending on the inlet conditions; intermediate sonic layer (h) formed between the subsonic region (f) and the supersonic region (g); and the detonation products are expanded azimuthally and axially to the exit plane.

A closeup view of the detonation wave front and the region around the wave front is given in Fig. 4 for various fields in order to comprehend the detonation wave structure along with other interesting phenomena. Each frame covers a spatial region of 0.2 × 0.2 in the axial and transverse directions, respectively. From the temperature and pressure field, we note that there is a high pressure zone in front of the heat release area. Moreover, a classical detonation wave structure can be seen from the azimuthal and axial velocity plot.

To determine if the flow field within the RDE had stabilized, we looked at the temporal evolution of the pressure regularity along the centerline in the detonation wave front. Fig. 5 shows that the flow field acquired its stability criteria after a small fluctuation. In addition, the zoom in picture of Fig. 5 illustrates a sequential pressure regularity in the flow field behavior.

4.2 Grid resolution study

The theoretical and numerical framework outlined in the preceding sections is used to analyze 2-D detonation phenomenon in various regimes. Because of limited computational resources, only seven grids (38 × 38, 76 × 76, 151 × 151, 301 × 301, 601 × 601, 1201 × 1201, and 2001 × 2001), with grid sizes as summarized in Table 1, were considered for the case of k = 2000, in order to precisely address the issue of grid resolution. Fig. 6 shows a smoke-foil record for different grids. A smoke-foil record can be numerically reproduced based on the domain peak pressure [6]. For coarse grids (151 × 151 and 301 × 301), the particle fluctuation is not sufficiently captured with the appropriate grid size. However, as the grid becomes finer (1201 × 1201 and 2001 × 2001), a cross sectional wave pattern was obtained that clearly shows the detonation cell structures. In the fine grid, the cell sizes are smaller near the head wall due to the triple shock collision with the solid wall, whereas the cell sizes are larger on the unconfined side.

In the case of a detonation wave simulation with a simplified reaction model, an experimental comparison can be made by changing the pre-exponential factor (k) value, which has a physical scaling factor of reaction speed, since the k value can be tuned either by comparison with the experimental detonation cell size or with a one-half reaction length. Thus, the experimental comparison has no great significance, but the effects of other flow and thermo-chemical parameters are typically investigated in this sort of study. The validity of the present modeling procedure was thoroughly studied in [21], and most of the previous detonation studies used these types of simplified models [11, 13, 15, 17]. Recent studies [3-6, 8, 22, 31, 32] have used this approach for the investigation of combustion characteristics in RDEs, which gave good comparisons with experimental observations and physical insights into RDEs. The present results exhibit general agreement with previous RDE studies. The k value was tuned accordingly for comparison with the experimental detonation cell size provided by Austin [34]. Basically, the k value is related to its dimensional counterpart (k*) through the time scale $\left(\frac{L^*}{u^*}\right)$. If k* and the velocity scale

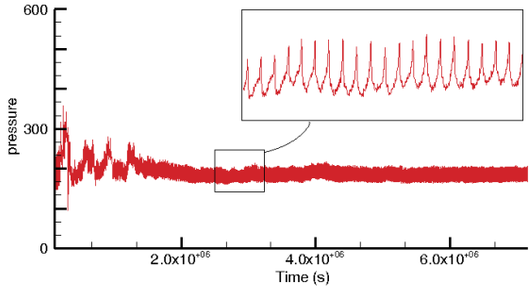

Fig. 5. Temporal variation of pressure along the centerline in the detonation wave front (2001 × 2001, θ = 5.2, k = 2000, Δ x = 0.00125).

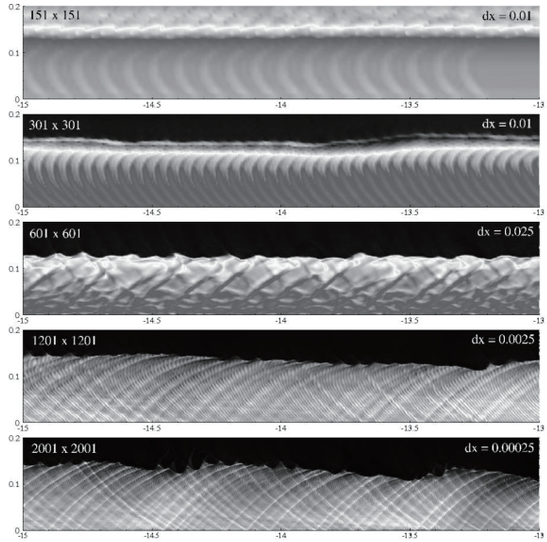

Fig. 6. Numerical smoke foil records for different grids (θ = 5.2, k = 2000).

(u*) are fixed, then k is proportional to the physical length scale used [21].

The detonation cell size of the $2H_2 + O_2 + 12Ar$ mixture (r_1 = 1.60, r_2 =1.29, MW = 34.4) is estimated by Austin at initially 20 kPa and 298 K [34]. The detonation cell size from the smoked-foil record is considered to be a characteristic dimension. The initial reference conditions used for their experiment are given in Table 2 with the nondimensional values.

By considering the reference as a ten-cell size width, the experimental smoked-foil records are 60 mm. From this numerical simulation, the typical ten-cell size shown in Fig. 6(e) is approximately 0.45L*. This yields L* = 133.3 mm, which corresponds to an RDE diameter of 63.67 mm. This is small considering a realistic engine size and operating conditions, but is considered to be sufficient to understand the wave front structures and dynamics of an RDE. In realistic operational conditions, the detonation cell size would be much smaller than that of the present study, which need finer resolution and lot of computation cost to resolve it.

The grey scale contour shown in Fig. 6(e) exhibits a fairly regular pattern of interacting transverse waves that closely resembles the open-shutter photograph of a detonation in a thin channel by Lee [35]. The numerical results are also consistent with the experimental observations that the detonation cell size is smaller near the upstream region, but decreases in initial pressure toward the downstream, resulting in a larger cell width [34].

Detonation properties of an elected stream trace for several numerical cases are shown in Fig. 7. The minimum grid size required to achieve detonation is 38 × 38, and no detonation occurs for a grid size of 30 × 30. Apart from the very low grid cases, there is no large variation in the flow field features for other higher-order grids, which shows that the flow field characteristics are less dependent on the grid resolution. For instance, the time taken for the coarse grid (151 × 151) to perform 60,000 iterations (to reach the quasi-steady state condition) is 8 min, which is 6473.2 min less than the fine grid (2001 × 2001) simulation. Therefore, in the interest of calculating detonation properties, coarse grids provide a much more computational time and resource saving option than the fine grids. Fig. 8 shows the

Table 2. Initial reference conditions used for Austin's experiment [34] with the nondimensional values used in the present study

Quantities	Reference values [34]	Nondimensional values
Pressure (p)	20 kPa	0.77
Temperature (T)	298 K	0.77
Detonation velocity	1517.9 m/s	5.656
Pre-exponential factor (k*)	5.2 x10^6 1/s	2000
Heat release (q)	2.32 kJ/kg	24.2

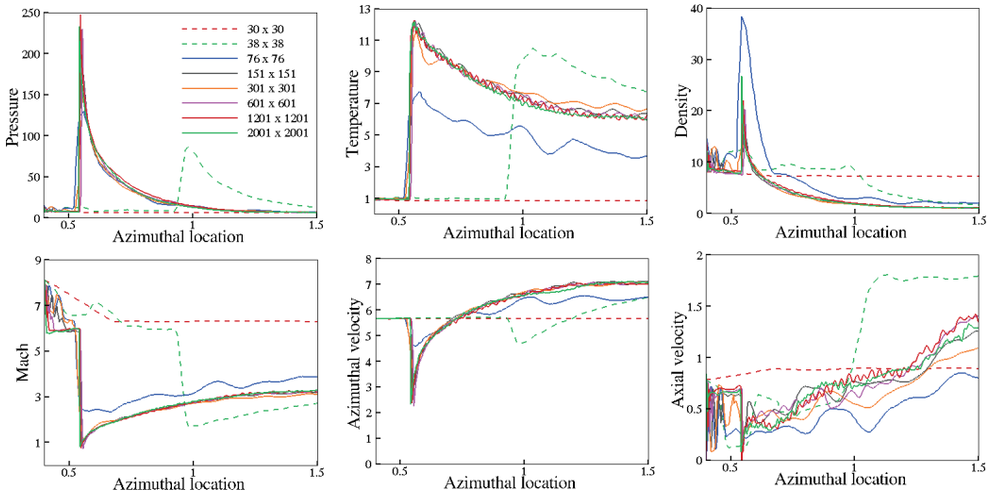

Fig. 7. Detonation flow properties of a stream trace for different grids (θ = 5.2, k = 2000).

DOI: http://dx.doi.org/10.5139/IJASS.2015.16.4.548

temperature contours for different grids, thus demonstrating that the detonation properties are less dependent on the grid size. Fig. 9 also shows the pressure and density variations of a particular particle moving from the inlet to an outlet for different grids in such a way as to lend support for the conclusions suggested in Fig. 7.

4.3 Propulsive performance analysis

4.3.1 Nonuniform exhaust flow

We considered the efficiency loss due to nonuniform flow at the outlet. Fig. 10(a) presents the temperature contour with streamlines (in black) throughout the annulus of an "unwrapped" RDE. It is possible that the large numbers of particles push off directly through the exit plane after going through the detonation wave front. On the other hand, some particles drive into the oblique shock created by the detonation waves, and then move out of the plane in a substantially divergent state. Fig. 10(b) represents the mass flow variation along the inlet and outlet of the computational domain. We note that the fluctuation is significant at the exit near the oblique shock region. This kind of particle nonuniformity affects the performance of the system, which ought to be controlled by reducing the mass flow through the generated oblique shock waves.

4.3.2 Effect of the number of detonation waves

Yi et al. proposed that an RDE delivers almost the same performance when increasing the number of detonation waves [6]. Fig. 11 shows temperature contours of detonation waves in a one-waved, three-waved, and four-waved RDE with respective pre-exponential factors of k = 10000, 20000, and 30000, with baseline injection conditions. The height of the detonation wave front is higher for a reduced k value of 10000, and when the k value increased, the detonation height decreased. In addition, the number of shock waves

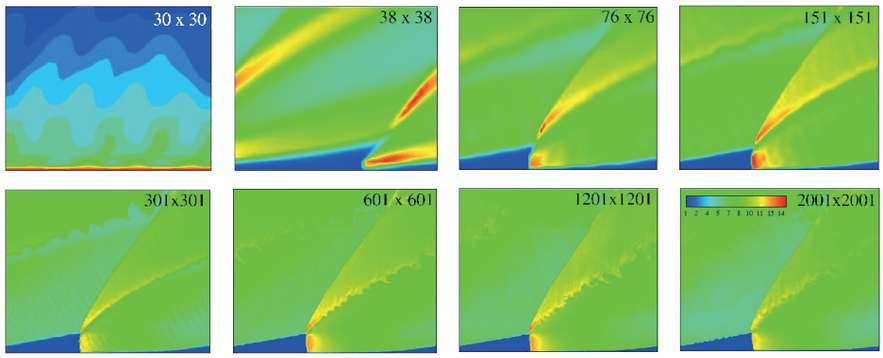

Fig. 8. Temperature contours for different grids (θ = 5.2, k = 2000)

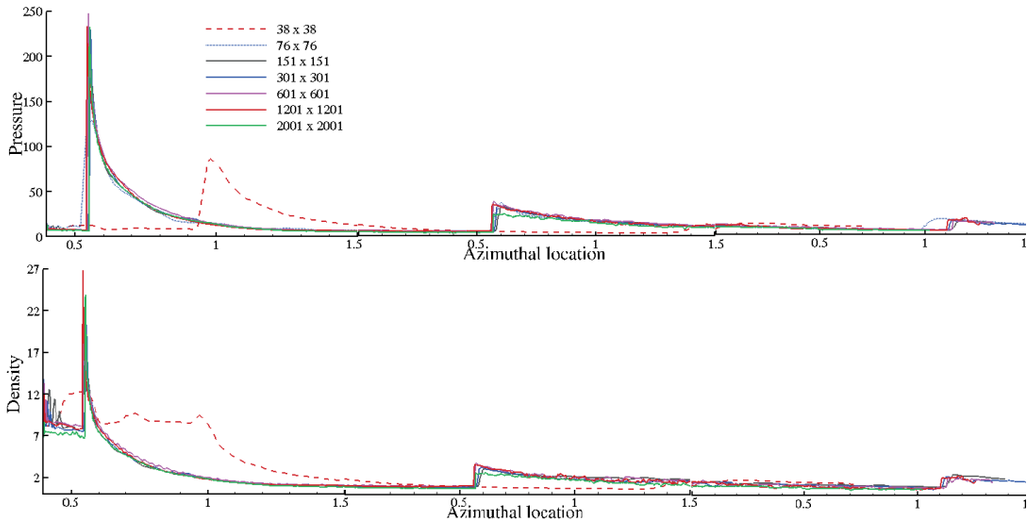

Fig. 9. Pressure and density variation showing the full stream trace of a particle throughout the domain for different grids (θ = 5.2, k = 2000).

generated in the case of a larger k value increased but the waves were weaker, which does not significantly affect the uniformity of the exit mass flow. However, even though a single oblique shock wave was generated with the lower k value, the strength is impressive. This does affect the uniformity of the exit mass flow, which in turn affects the system's performance, as mentioned in the previous section. In future work, further examination of the performance of particle fluctuations related to thrust potential and specific impulse is needed.

4.4 Flow field physics in the detonation wave front

Detonation features and flow field behavior of stream traces passing through the detonation wave front is of great concern in rotating detonation engine simulations. Fig. 12 shows the pressure field with four picked stream traces piercing the detonation wave front via the nethermost portion (a), halfway point (b), two-thirds distance (c), and apex portion (d) of the detonation wave front. Physical properties of those streamlines were extracted and correlated as shown in Fig. 13. From the XY chart, it appears possible that the bottom-most streamlines, known as the stream trace, (a) has zenithal pressure and diminished fluctuations, whereas stream trace (d) has intensified variations with low set pressure values because of interaction with the procreated oblique shock waves.

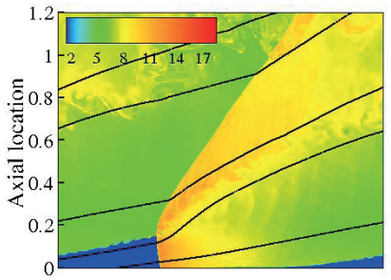

(a)

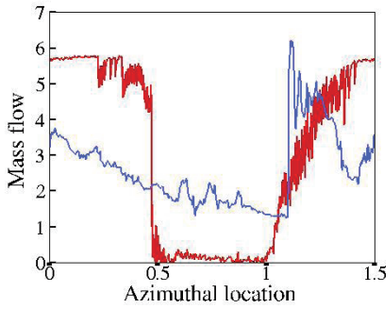

(b)

Fig. 10. (a) Temperature contour with streamlines, and (b) mass flow variation on the inlet (red) and outlet (blue) along the azimuthal location (2001 × 2001, θ = 5.2, Δ x = 0.00125).

4.5 Tertiary shock wave pattern

Figure 14 juxtaposes the pressure contour for different grids to distinguish the tertiary shock strength across the domain. For coarse grids, the tertiary shocks behind the detonation wave front are thicker and less in number. Nevertheless, for fine grids, tertiary waves are thin and skimpy. The detonation front curvature is greater for the coarse grids than for the fine grids.

We also scrutinized the tertiary shock wave in the flow field because of the prevailing regional supersonic flow behind the diffracting shocks. In Fig. 15, we assimilated the pre-exponential factor k for several cases (2000, 5000, and 10000) and examined the axial velocity, which clearly displays the

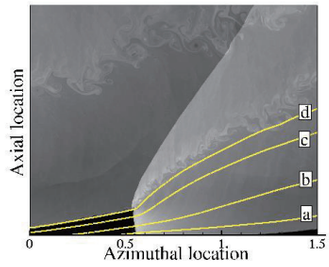

Fig. 12. Pressure flow field with stream traces of a flow particle (2001 × 2001, θ = 5.2, Δ x = 0.00125).

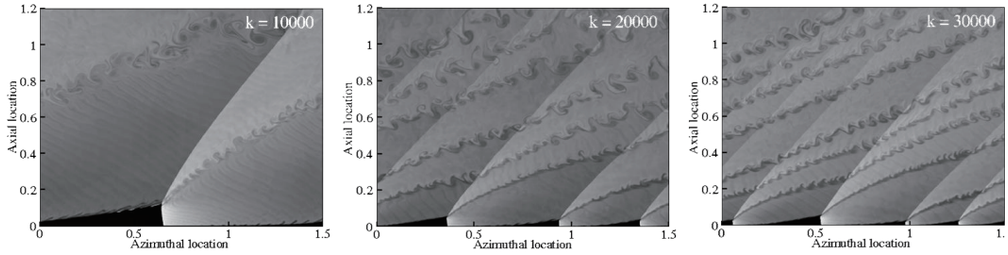

Fig. 11. Temperature gradient of detonation waves in one-, three-, and four-waved RDE (1201 × 1201, θ = 5.2, Δ x = 0.0025).

DOI: http://dx.doi.org/10.5139/IJASS.2015.16.4.548

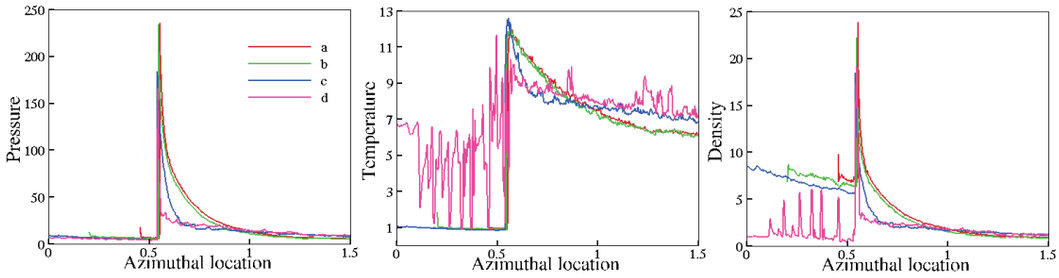

Fig. 13. Variation in the flow field properties captured using stream traces (2001 × 2001, θ = 5.2, Δ x = 0.00125).

wave patterns. We whited out the area ahead of the oblique shock to untangle how this region is affected by modifying the k value. Shock wave interaction is weak for a reduced k value. However, as k is increased, the interaction becomes stronger and more forcible, which is due apparently to the formation of cell structures in front of the oblique shock. All of the gas particles within the walls of the domain are treated through these shock waves, and thus they will have a performance loss associated with them.

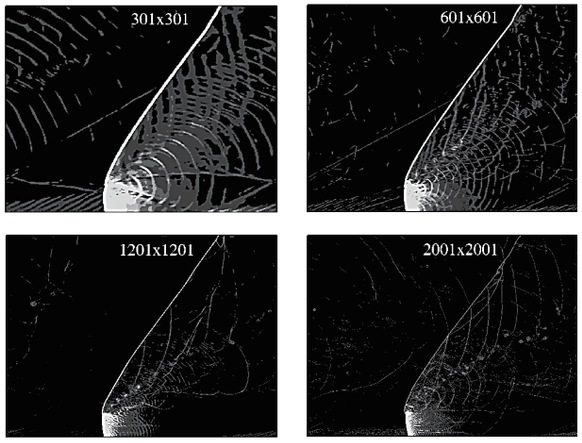

Fig. 14. Pressure gradient contours for different grids showing the tertiary shock waves (θ = 5.2, k = 2000)

5. Conclusion

We performed a 2-D numerical simulation of an unsteady Euler's equation with a one-step chemical reaction to study stationary detonation wave front propagation in an annular chamber of an unwrapped RDE. A quasi-steady state simulation was used to investigate the effect of grid size in producing detonation cell structure, and the performance impact of nonuniform exit mass flow. Additional work examined the detonation wave physics and tertiary shock formations. In conclusion, time-efficient calculations in performance and flow field behavior were obtained using quasi-steady state simulation. We also identified that flow particle fluctuation is the main problem for performance losses, which can be decreased by controlling and regulating the same amount of mass entering through the oblique shock waves. A thorough study of particle fluctuation needs to be carried out in future work.

Acknowledgement

This work has been carried out by the Advanced Research Center Program (No. 2013073861) contracted through Advanced Space Propulsion Center at Seoul National

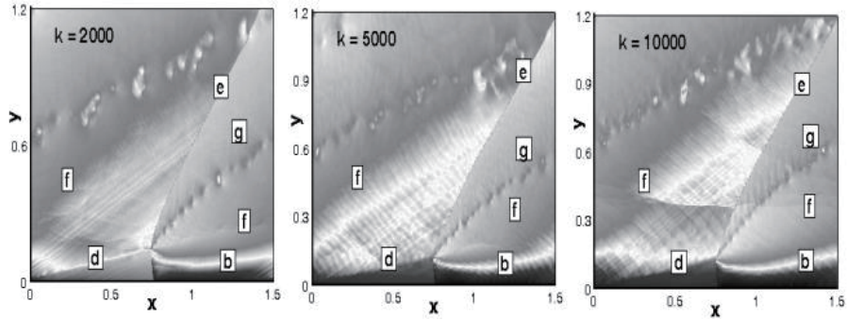

Fig. 15. Tertiary shock waves formed in front of oblique shock waves for different pre-exponential factors (2001 × 2001, θ = 5.2, Δ x = 0.00125).

University and the National Space Lab Program (NRF-2013M1A3A3A02042430), both supported by the National Research Foundation of Korea (NRF) grant funded by the Korea Government (Ministry of Science, ICT and Future Planning).

References

[1] Tsuboi, N., Yamada, T., Hayashi, A. K. and Yamada, E., "Three Dimensional Simulation on a Rotating Detonation Engine: Three Dimensional Shock Structure", *4th International Symposium on Energy Materials and their Applications*, Japan, 2011.

[2] Braun, E. M., Lu, F. K., Wilson, D. R. and Camberos, J. A., "Air Breathing Rotating Detonation Wave Engine Cycle Analysis", *Aerospace Science and Technology*, Vol. 27, Issue 1, 2013, pp. 201 - 208. DOI:10.1016/j.ast.2012.08.010

[3] Davidenko, D., Eude, Y., Go¨kalp, I. and Falempin, F., "Theoretical and Numerical Studies on Continuous Detonation Wave Engines", *Detonation Wave Propulsion Workshop*, Bourges France, 11 – 13 July 2011.

[4] Zhou, R. and Wang, J. P., "Numerical Investigation of Flow Particle Paths and Thermodynamic Performance of Continuously Rotating Detonation Engines", *Combustion and Flame*, Vol. 159, Issue 12, 2012, pp. 3632 - 3645.
DOI:10.1016/j.combustflame.2012.07.007

[5] Eude, Y. and Davidenko, D., "Numerical Simulation and Analysis of a Three Dimensional Continuous Detonation under Rocket Engine Conditions", *Detonation Wave Propulsion Workshop*, Bourges France, 11 – 13 July 2011.

[6] Yi, T. H., Lou, J., Turangan, C., Choi, J. Y., Wolanski, P., "Propulsive Performance of a Continuously Rotational Detonation Engine", *Journal of Propulsion and Power*, Vol. 27, Issue. 1, 2011, pp. 171 – 181. DOI: 10.2514/1.46686

[7] Naour, B. L., Falempin, F. and Miquel, F., "Recent Experimental Results obtained on Continuous Detonation Wave Engine", *Detonation Wave Propulsion Workshop*, Bourges France, 11 – 13 July 2011.

[8] Davidenko, D., Jouot, F., Kudryavtsev, A., Dupre, G., Go¨kalp, I., Daniau, E. and Falempin, F., "Continuous Detonation Wave Engine Studies for Space Application", *European Conference for Aeronautics and Space Sciences Proceedings Series*, Vol. 1, 2009, pp. 353 - 366. DOI:10.1051/eucass/200901353

[9] Endo, T., Susa, A., Kanekiyo, K., Hanta, Y., Mitsunobu, A. and Takahashi, T., "Development of Pulse Detonation Technology in Valveless mode and its Application to Turbine Drive Experiments", *International Workshop on Detonation for Propulsion*, South Korea, 14 – 15 November 2011.

[10] Oran, E. S., Boris, J. P., Young, T., Flanigan, M., Burks, T. and Picone, M., "Numerical Simulations of Detonations in Hydrogen-Air and Methane-Air Mixtures", *18th International Symposium on Combustion*, Vol. 18, Issue 1, 1981, pp. 1641 - 1649. DOI:10.1016/S0082-0784(81)80168-3

[11] Taki, S. and Fujiwara, T., "Numerical Simulation of Triple Shock behavior of Gaseous Detonation", *18th International Symposium on Combustion*, Vol. 18, Issue 1, 1981, pp. 1671 – 1681. DOI:10.1016/S0082-0784(81)80171-3

[12] Kailasanath, K., Oran, E. S., Boris, J. P., and Young, T. R., "Determination of Detonation Cell Size and the Role of Transverse Waves in Two Dimensional Detonations," *Combustion and Flame*, Vol. 61, Issue 3, 1985, pp. 199 - 209.
DOI:10.1016/0010-2180(85)90101-4

[13] Bourlioux, A. and Majda, A. J., "Theoretical and Numerical Structure for Unstable Two Dimensional Detonations," *Combustion and Flame*, Vol. 90, Issues 3 - 4, 1992, pp. 211 - 229. DOI:10.1016/0010-2180(92)90084-3

[14] Oran, E. S., Weber, J. W., Stefaniw, E. I., Lefebvre, M. H. and Anderson, J. D., "A Numerical Study of a Two-Dimensional H2-O2-Ar Detonation Using a Detailed Chemical Reaction Model," *Combustion and Flame*, Vol. 113, Issues 1-2, 1998, pp. 147 – 163. DOI:10.1016/S0010-2180(97)00218-6

[15] Gamezo V. N., Desbordes, D. and Oran, E. S., "Formation and Evolution of Two-Dimensional Cellular Detonations," *Combustion and Flame*, Vol. 116, Issues 1 - 2, 1999, pp. 154 - 165. DOI:10.1016/S0010-2180(98)00031-5

[16] Gavrikov, A. I., Efimenko, A. A. and Dorofeev, S. B., "A Model for Detonation Cell Size prediction from Chemical Kinetics," *Combustion and Flame*, Vol. 120, Issues 1-2, 2000, pp. 19-33. DOI:10.1016/S0010-2180(99)00076-0

[17] Sharpe, G.J., "Transverse Waves in Numerical Simulations of Cellular Detonations," *Journal of Fluid Mechanics*, Vol. 447, 2001, pp. 31 - 51.
DOI: http://dx.doi.org/10.1017/S0022112001005535

[18] Hu, X. Y., Khoo, B. C., Zhang, D. L. and Jiang, Z. L., "The Cellular Structure of a Two-Dimensional H2/O2/Ar Detonation Wave," *Combustion Theory and Modelling*, Vol. 8, Issue 2, 2004, pp. 339 - 359.

[19] Liang, Z. and Bauwens, L., "Cell Structure and Stability of Detonations with a Pressure-dependent Chain-branching Reaction Rate Model," *Combustion Theory and Modelling*, Vol. 9, Issue 1, 2005, pp. 93 - 112.

[20] Fickett, W. and Davis, W.C., *Detonation: Theory and Experiment*, Dover Publications, Inc., Mineola, New York, 1979.

[21] Choi, J. Y., Ma, F. H. and Yang, V., "Some Numerical Issues on Simulation of Detonation Cell Structures", *Combustion, Explosion, and Shock Waves*, Vol. 44, Issue 5,

2008, pp. 560 - 578.

[22] Hishida, M., Fujiwara, T. and Wolanski, P., "Fundamentals of Rotating Detonations", *Shock waves*, Vol. 19, Issue 1, 2009, pp. 1 - 10.

[23] Voitsekhovskii, B. V., "About Spinning Detonation", *Dokl. Akad. Nauk SSSR*, Vol. 114, 1957, pp. 717 - 720.

[24] Voitsekhovskii, B.V. and Kotov, B.E., "Optical Investigation of the Front of Spinning Detonation Wave", *Izv. Sibirsk. Otd. Akad. Nauk SSSR*, Vol. 4, 1958.

[25] Cullen, R. E., Nicholls, J. A. and Ragland, K.W., "Feasibility Studies of a Rotating Detonation Wave Rocket Motor", *Journal of Spacecraft and Rockets*, Vol. 3, Issue 6, 1966, pp. 893 - 898.

[26] Nicholls, J. A., Wilkinson, H. R. and Morrison, R. B., "Intermittent Detonation as a Thrust-Producing Mechanism", *Journal of Jet Propulsion*, Vol. 27, Issue 5, 1957, pp. 534 - 541.
DOI: 10.2514/8.12851

[27] Bykovskii, F. A., Vasil'ev, A. A., Vedernikov, E. F. and Mitrofanov, V. V., "Explosive Combustion of a Gas Mixture in Radial Annular Chambers", *Combustion, Explosion and Shock Waves*, Vol. 30, Issue 4, 1994, pp. 510 - 516.

[28] Bykovskii, F. A., Vasil'ev, A. A. and Vedernikov, E. F., "Continuous Spin Detonation of Fuel-air Mixtures", *Combustion Explosion and Shock Waves*, Vol. 42, Issue 4, 2006, pp. 463 - 471.

[29] Daniau, E., Falempin, F. and Zhdan, S., "Pulsed and Rotating Detonation Propulsion Systems: First Step toward Operational Engines," *AIAA/CIRA 13th International Space Planes and Hypersonics Systems and Technologies*, 2005.

[30] Falempin, F. and Daniau, E., "A Contribution to the Development of Actual Continuous Detonation Wave Engine", *15th AIAA International Space Planes and Hypersonics Systems and Technologies Conference*, 2008.

[31] Hayashi, A. K., Kimura, Y., Yamada, T., Yamada, E., Kindracki, J., Dzieminska, E., Wolanski, P., Tsuboi, N., Tangirala, V. and Fujiwara, T., "Sensitivity Analysis of Rotating Detonation Engine with a Detailed Reaction Model", *47th AIAA Aerospace Sciences Meeting Including The New Horizons Forum and Aerospace Exposition*, 2009

[32] Schwer, D. and Kailasanath, K., "Numerical Investigation of the Physics of Rotating Detonation-Engines", *Proceedings of the Combustion Institute*, Vol. 33, Issue 2, 2011, pp. 2195 - 2202.
DOI:10.1016/j.proci.2010.07.050

[33] Claflin, S., "Recent Progress in Rotating Detonation Engine Development at Aerojet Rocketdyne", *International Workshop on Detonation for Propulsion*, Taiwan, 2013.

[34] Austin, J. M., "The Role of Instability in Gaseous Detonation", *Thesis Dissertation, California Institute of Technology*, California, 2003.

[35] Lee, J. H. S., "The Detonation Phenomenon", Cambridge University Press, New York, 2008.